ACS OMEGA

Open Access

http://pubs.acs.org/journal/acsodf

Article

Synthesis and Characterization of Thermostable Antimicrobial Peptide−DNAzyme Conjugates for the Proof-of-Concept Detection of *E. coli*

Natalie Mutter, Filippo Savini, Željka Ban, Dijana Pavlović Saftić, Andrea Hloušek-Kasun, Yasaman Ahmadi, Branimir Bertoša, Ivo Piantanida,* and Ivan Barišić*

Cite This: *ACS Omega* 2026, 11, 8024−8033

Read Online

ACCESS | Metrics & More | Article Recommendations | Supporting Information

ABSTRACT: Bacterial infections are a common cause of morbidity and mortality worldwide. The early detection of pathogens is crucial to minimize health risks, control spread, and prevent outbreaks. Current detection methods are either cultivation-based and time-consuming or rely on sophisticated, costly assays that require specialist equipment, making them unsuitable for rapid and cost-efficient screening, e.g., in food safety. Here, we investigated antimicrobial peptides (AMPs) conjugated to HRP-mimicking DNAzymes as a potentially novel class of broad-spectrum bacterial biosensors. AMPs bind to bacterial cells, and the DNAzyme catalyzes a peroxidase reaction exploitable for sensing applications. We established and optimized a synthesis protocol to prepare AMP-DNAzyme conjugates, synthesized several AMP/DNAzyme combinations, and characterized them. Molecular dynamics simulations of selected conjugates were conducted to gain insight into their binding capacity. We also investigated the potential of these constructs for the proof-of-concept detection of a clinical*Escherichia coli*isolate on two low-cost detection platforms: a syringe microfilter system and an ELISA-like assay. On the syringe microfilter, we detected 10^8 cells/mL within 30 min, while the ELISA-like assay achieved a limit of detection below 5 cells/mL, resulting in 1−2 orders of magnitude improved sensitivity compared to similar AMP-based biosensors. This highly stable and cost-efficient biosensor can have potential applications in fields such as environmental monitoring, food safety, and quality control, where a broad approach is used to detect the presence of bacterial contamination.

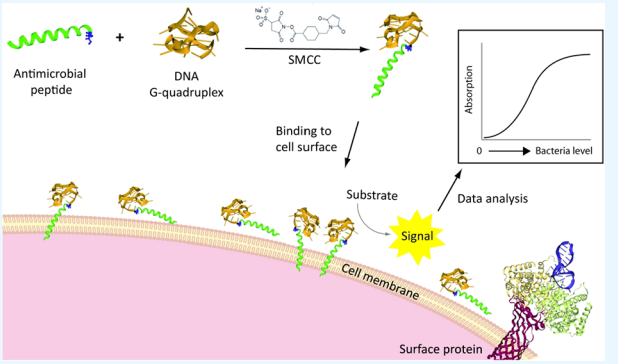

1. INTRODUCTION

Bacterial diseases represent a threat to human health and are annually responsible for over 7 million deaths worldwide.[1] Bacterial detection commonly involves either cultivation or molecular techniques. The gold standard is based on cultivation-based methods that are well established and cost-effective. However, the cultivation of some pathogens is challenging and time-consuming, taking in some cases even weeks.[2] In contrast, molecular methods, such as polymerase chain reaction, can identify bacteria within hours but are expensive and require highly skilled personnel. Both approaches are not optimal for certain health threat scenarios, such as food safety, where bacterial contamination must be detected rapidly and cost-efficiently. Thus, there is an increasing demand for the development of novel methods for the cost-effective and rapid detection of pathogenic bacteria.

AMPs are small peptides produced by all living organisms as a first line of defense against pathogens.[3,4] The majority of known AMPs are short and amphipathic. Cationic peptides bind selectively to the anionic membranes of bacterial cells[5,6] and lyse the cells by perturbating the bacterial membrane. Due to their high affinity to bacterial surfaces, AMPs are becoming increasingly interesting as biorecognition elements in biosensors.[7−11] In addition to the relatively low costs compared with globular proteins, their main advantage is the very high stability. Their binding capability can be restored even after boiling or autoclaving.[12] Furthermore, their small size enables spatially dense biosensor surfaces, which positively impacts the sensitivity in certain sensor setups.[13,14] To fully exploit these unique properties, the signal generating unit should feature the same advantages. To achieve this, we used a DNA-based reporter enzyme (DNAzyme). The guanine-rich oligonucleotides can fold into stable four-stranded structures known as G-quadruplexes (G4), in which four guanine bases are hydrogen-

Received: October 3, 2025
Revised: December 15, 2025
Accepted: December 19, 2025
Published: January 27, 2026

https://doi.org/10.1021/acsomega.5c10306
ACS Omega 2026, 11, 8024−8033

Scheme 1. Strategies of DNA Tethering with Bacteria Binding Peptides[a]

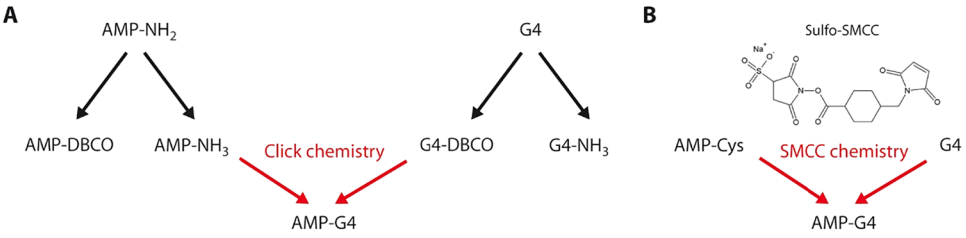

[a](A) Modifications of AMP amino groups followed by SPAAC click reaction with activated DNA molecules; (B) SMCC reaction of AMP thiol group and activated DNA molecules.

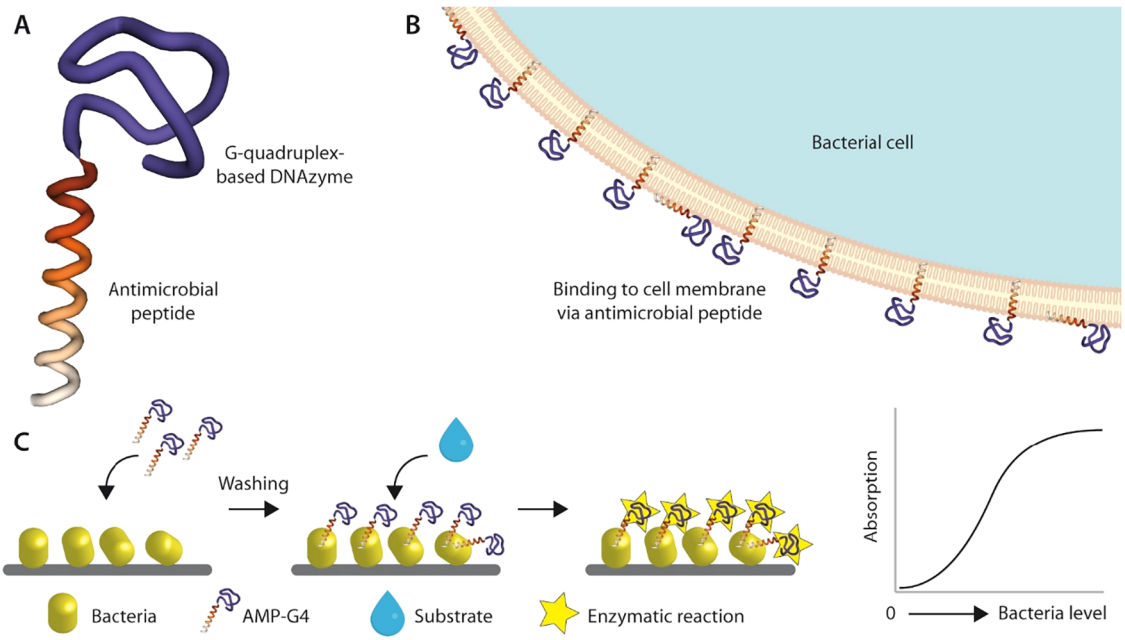

Figure 1. (A) Structural model of an AMP-G4 conjugate generated in Catana.[25] (B) Model of the AMP-G4 binding to the cell. The conjugates bind to the cell membrane and cover the cell surface. In contrast to free AMP,[26] the conjugates cannot easily form barrels and pores that disrupt the membrane due to steric hindrance caused by the G4. This effect leads to reduced or even no antimicrobial activity (Table S3). This is a key feature of our technology and is essential to achieve a high sensitivity since lysed cells and their fragments are washed away together with the targeting and reporter molecules. (C) Scheme of the detection principle. Bacterial cells are incubated with AMP-G4. After a washing step, the substrate is added, and the enzymatic activity is measured via absorbance.

bonded to each other to form a planar arrangement known as the G-tetrad.[15,16] The G4 complex with hemin mimics the protein-based horseradish peroxidase (HRP) activity, catalyzing the H_2O_2-mediated oxidation of various substrates, such as TMB and Amplex Red. By covalently conjugating the G4 (as HRP-mimicking DNAzyme in complex with hemin) to AMPs, a novel and highly robust class of biosensors was realized that retained its binding and reporting activity even after a 90 °C heating step. The catalytic activity of a DNAzyme is considerably less than its protein analogues. In a previous study, we compared the kcat (turnover number) values of the used PS2.M G4/hemin ($34 \pm 3\ s^{-1}$) and the HRP enzyme ($1.65 \pm 0.09) \times 10^5\ s^{-1}$.[17] Despite the lower activity, DNAzymes offer several advantages compared with protein-based enzymes. These include chemical and thermally stability, easy synthesis, and the possibility to readily conjugate them to various molecules, such as fluorescent tags, solid surfaces, or peptides, allowing the adaptation for diverse detection formats.[18] In addition, the very popular horseradish peroxidase (HRP) features strong unspecific binding to various surfaces leading to significant background signals, which limits the sensitivity of assays.[19]

Several previous works employed either AMPs or DNAzyme as the main component of their biosensing platform.[18,20] Herein, we leveraged the potential of these two by combining them into one single, highly thermostable biosensor. Other alternative biorecognition elements to AMPs are antibodies, proteins, and aptamers, which were also used together with DNAzymes for developing biosensors. For example, Guo et al. developed an antibody-mediated electrochemical sensing system for the detection of *E. coli*, where the G4 DNAzyme was used as the detection element.[21] However, the significantly lower thermal stability of antibody-based components compared to AMP makes this system less stable. In addition, in that work, a polymerase was added to amplify the G4 sequence, making the system more complex compared to our study. Another example is a recent study by Pang et al., in which an exonuclease-assisted colorimetric sensor composed of G4 DNAzyme and aptamer was developed for detecting *E. coli* O157:H7.[22] While aptamers bind with high affinity and specificity to a wide range of targets, the binding affinity of

https://doi.org/10.1021/acsomega.5c10306
ACS Omega 2026, 11, 8024−8033

many aptamers strongly depends on the buffer composition (particularly ions), which cannot be easily exchanged in complex biological sample matrices.[23] In contrast, AMPs were evolutionary optimized to bind within various biological matrices.

The synthesis and characterization of peptide-nucleic acid conjugates, however, have proven to be difficult mainly due to the electrostatic interactions between the cationic peptide and the anionic DNA. To evaluate the diagnostic potential of AMP-G4 conjugates, first, we had to establish a simple but robust synthesis protocol for the chemical conjugation of different G4 sequences to a variety of different AMPs (Table S2). We selected two different G4 (AGRO100[15] and PS5.M,[16] Table S1), which bind to hemin and then exhibit an effective peroxidase-like activity. While other studies usually focus on a single AMP in their biosensors, we opted to investigate the modularity of our approach and selected four different AMPs for our study. First, we used a Cu-free click chemistry (strain-promoted alkyne−azide cycloaddition, SPAAC) approach for linking AMPs and G-rich DNA sequences (Scheme 1A).[24] This approach was based on the modification of DNA or AMP amino groups. However, due to the abundance of primary amines in peptides (lysine amino acids and N-terminus), such DNA-peptide coupling could result in heterogeneous mixtures of conjugates containing several DNA strands per peptide, which could affect the AMP-based bacteria recognition. An alternative approach relied on the site-specific reaction of a peptide thiol group and DNA using a SMCC bifunctional reagent (Scheme 1B), a very popular cross-linking agent for the maleimide modification of DNA and further reaction with peptide thiols. This approach was based on the activation of the DNA amino group with the bifunctional cross-linker sulfo-SMCC, followed by a reaction with peptide cysteine (thiol group). After establishing an optimal synthesis protocol, we used molecular dynamics simulations to obtain more information about the structural and dynamic properties of our peptide-DNA conjugates and their theoretical potential to bind to bacterial cells. Finally, we investigated the use of AMP-G4 DNAzyme conjugates as broad-spectrum bacterial biosensors for diagnostic applications (Figure 1). First, a portable method based on syringe microfilters was used for rapid, low-cost detection. Subsequently, a highly sensitive ELISA-like assay was developed to detect very low concentrations of pathogens.

2. MATERIALS AND METHODS

2.1. Folding of AMP-G4 Conjugates

The AMP−G4 stock solutions were stored at −20 °C and thawed prior to each experiment conducted over several months. Because AMP−G4 peroxidase activity was critical for the study, its effectiveness was tested before each new experiment and was found to remain consistent with the original sample. In addition, SDS analyses performed during this period confirmed the continued presence of AMP−DNA. Any potential chemical degradation or physical alteration, such as aggregation, would have been reflected in both the peroxidase activity and the SDS results. Therefore, the AMP−G4 conjugates demonstrated good stability under the applied storage conditions over several months. The AMP-G4 constructs were diluted to 20 μM in PBS and then incubated at 90 °C for 5 min. The AMP-G4 were cooled slowly 1 °C per minute, followed by addition of 50 μM KCl and incubated at room temperature for 40 min. Last, 10 μM hemin (stock 5 mM in DMSO) was added and kept at room temperature for 2 h. G4 folding was examined by measuring UV/vis spectroscopy and observing a new peak at 410 nm, corresponding to incorporated hemin.

2.2. TMB Activity Assay

The peroxidase activity assay reaction mixture contained 5 μM AMP-G4 and 10 μL of TMB solution (1-step ultra TMB-ELISA substrate solution, Thermo Fisher Scientific, Waltham, MA, USA) in PBS with a total volume of 100 μL. Immediately after adding the substrates, the reaction was followed by measuring absorbance at 605 nm at RT using a microplate reader (SpectraMaxi iD3Molecular Devices, Munich, Germany).

2.3. Filter Experiments

Bacterial cells were grown overnight in a 2xYT medium. The next day, the cells were adjusted to an OD_{600} of 1 using PBS. This corresponds to a concentration of ca. 10^9 cells/mL. Different bacterial dilutions in PBS were prepared. The filters were prewetted with 1 mL of PBS, and then 1 mL of each bacterial concentration was applied on a syringe filter composed of a polypropylene (PP) membrane with 0.22 μm. Then, the filter was washed with 5 mL of PBS. The AMP-G4 was diluted to 100 nM in PBS, and 250 μL was applied on the filter. After 5 min incubation at RT, the filters were washed with 5 mL of PBS. Finally, 250 μL of TMB substrate solution (1-step ultra TMB-ELISA substrate solution, Thermo Fisher Scientific, Waltham, MA, USA) was passed through each filter. The filters were incubated for 10 min at RT, before the development of blue color was observed, and a picture was taken.

2.4. Minimal Inhibitory Concentration (MIC)

The minimum inhibitory concentration (MIC), the most commonly used measure of antimicrobial peptide activity, was determined by adapting the microbroth dilution method, using sterile 96-well plates. Aliquots (50 μL) of bacteria in mid logarithmic phase at a concentration of 2×10^6 CFU/mL in culture medium (Mueller-Hinton, MH) were added to 50 μL of MH broth containing the peptide in serial 2-fold dilutions. The MIC was expressed as the minimum concentration of peptide at which 100% inhibition of microbial growth is visually observed after 16−18 h of incubation at 37 °C.

2.5. Plate Experiments (Absorbance)

Bacterial cells were first grown overnight in a 2xYT medium. The next day, the cells were washed with PBS and adjusted to an OD_{600} of 1 (correlate to 10^9 cells/mL) in PBS, and 100 μL was immobilized in each well of a 96-well plate (Nunc Immuno MaxiSorp MicroWell 96-well solid plate, M9410, Thermo Fisher Scientific, Waltham, MA, USA). The plate was incubated overnight at 4 °C. The next day, the coated wells were washed with 2× 200 μL PBS followed by blocking with 200 μL of 3% bovine serum albumin (BSA) in PBS for 1.5 h at RT. Then, the wells were washed with 3× 200 μL of PBS supplemented with 0.05% Tween-20. The AMP-G4 conjugates were prepared in serial 2-fold dilution (0.07−5 μM) in PBS. A total of 100 μL of each AMP-G4 concentration was added per well. The plate was incubated for 1 h at room temperature, followed by washing the wells once with 200 μL of PBS and addition of 100 μL of TMB solution. Immediately afterward, absorbance was measured at 605 nm for at least 40 min using a

https://doi.org/10.1021/acsomega.5c10306
ACS Omega 2026, 11, 8024−8033

plate reader (SpectraMax iD3Molecular Devices, Munich, Germany).

2.6. Plate Experiments (Fluorescence)

Bacterial cells were first grown overnight in 2xYT medium. The next day, the cells were washed with PBS and adjusted to a OD_{600} of 1 (correlate to 10^9 cells/mL) or diluted to cell concentrations of $10-10^7$ cells/mL in PBS, and in all cases, 100 μL was immobilized in each well of a 96-well plate (Greiner flat clear bottom, black polystyrene 96-well plate, 10281092, Thermo Fisher Scientific, Waltham, MA, USA). The plate was incubated overnight at 4 °C. The next day, the coated wells were washed with 2× 200 μL PBS, followed by blocking with 200 μL of 3% BSA in PBS for 1.5 h at room temperature. Then, the wells were washed with 3× 200 μL of PBS supplemented with 0.05% Tween-20. The AMP-G4 conjugates were prepared either in serial 2-fold dilution (5−0.07 μM) in PBS and tested on 10^9 cells/mL or diluted to 5 μM and tested on varying cell concentrations. A total of 100 μL of each AMP-G4 concentration was added per well. The plate was incubated for 1 h at room temperature, followed by washing the wells twice with 200 μL of PBS. Then, 100 μL of the substrate solution was added, comprising 25 μM Amplex Red and 0.5 mM H_2O_2. The fluorescence was measured immediately afterward using an excitation wavelength of 530 nm and for emission wavelength of 590 nm and the low gain settings at the plate reader (SpectraMaxi iD3Molecular Devices, Munich, Germany).

3. RESULTS AND DISCUSSION

3.1. Synthesis of AMP-G4 Conjugates

AMPs are highly positively charged molecules, while DNA oligonucleotides are highly negatively charged. These properties, in combination with intramolecular folding, can lead to poor synthesis yields or even total failure of the reaction. Thus, two different synthesis strategies were evaluated for the generation of AMP-G4 conjugates, including (1) SAAP click chemistry and (2) a sulfo-SMCC conjugation method (Scheme 1).

3.1.1. SPAAC Click Chemistry. First, we used SPAAC, a Cu-free bioorthogonal reaction utilizing a pair of reagents, cyclooctynes, and azides that exclusively and efficiently react with each other through the formation of a stable triazole (Scheme S4A). AMPs with highly reactive amino groups (lysine and N-terminus amino group) can be functionalized with both azido and DBCO modifications. The AGRO100 and PS5.M DNA sequences were purchased with an amino group at the 5′-end for azido and DBCO modifications. Therefore, we explored both approaches, which were directed to give the same conjugate (Scheme S4B): (A) DBCO modification of AMP amino groups followed by SPAAC click reaction with azido-modified DNA, and (B) Azido modification of AMP amino groups followed by SPAAC click reaction with DBCO-modified DNA. More details on the experimental procedure and results can be found in the Supporting Information.

Both synthesis strategies were analyzed by SDS-PAGE electrophoresis and HPLC. The SDS-PAGE electrophoresis analysis confirmed mainly the presence of unreacted AMPs in the reaction mixtures and no formation of the desired products (Figure S1). HPLC analyses revealed the presence of the desired products, but the yield was too low for our diagnostic application. Therefore, we switched to an alternative synthesis approach.

3.1.2. Sulfo-SMCC Conjugation Method. The regioselective linking of DNA to an AMP can be also achieved by a 2-step procedure that includes a sulfo-SMCC reagent (Scheme S3), a water-soluble heterobifunctional cross-linker that contains N-hydroxysuccinimide (NHS) ester, and a maleimide group allowing covalent conjugation of amine- and sulfhydryl-containing molecules. This fragment conjugation strategy is limited to peptides that contain one cysteine residue per sequence, preferably at the N- or C-terminus, yielding site-specific complexes with DNA (1:1 conjugate).

We examined this site-specific approach for covalent conjugation of the amine-modified DNA sequences PS5.M and AGRO100 and cysteine-modified AMPs having one cysteine at the C-terminus (Table S2, *Experimental procedure* 3). Since the maleimide group is more stable than the NHS-ester group, conjugations with an NHS-ester (amine-targeted) have to be obtained before the maleimide (sulfhydryl-targeted) reaction. The sulfo-SMCC cross-linker was first reacted with the 5′ amino-modified oligonucleotide to produce a maleimide-activated DNA. Since thiols are prone to oxidative dimerization with the formation of disulfide bonds that do not react with maleimides, it is necessary to reduce the AMP disulfides prior to the conjugation. Therefore, the disulfide-reducing agent TCEP was used. TCEP should not react with the maleimide; therefore, purification was omitted. After purification of the excess cross-linker using centrifugal filters with a MW cutoff of 3,000, SMCC-DNA intermediate and an equimolar amount of reduced AMP were reacted to generate the final AMP-DNA conjugates. SDS-PAGE electrophoresis was used to visualize the progress of the ligation reactions (Figure S2).

The best results, meaning complete conversion of the starting AMP, were observed with the BMAP18 C peptide (Figure S2, lane 3) and GF17_His C peptide (Figure S2, lane 6). Those two AMP-DNA conjugates were heated to 90 °C (G4 folding), allowed to cool to ambient temperature, and then analyzed using UV/vis and circular dichroism (CD) spectroscopy (Figure S3). As the binding of G4 to hemin results in a clear hyperchromicity of the Soret band of hemin, the UV/vis absorption spectroscopy was utilized to study the interactions between hemin and different AMP-G4 conjugates. The BMAP18 C-PS5.M conjugate as well as GF17 His C-PS5.M were quantified using UV/vis absorption spectroscopy. The free hemin (not bound to DNA) has a Soret absorption band centered at λ = 379 nm (Figure S4A, green line). After incubation with G4 DNA, strong hyperchromicity and bathochromic shifts (to λ = 408 nm) are always observed for the hemin Soret band (Figure 4A, blue line). The same phenomenon was observed for the GF-17_His C-PS5.M conjugate (Figure S3B).

The CD profile of the BMAP18 C-PS5.M conjugate displayed a positive peak at 270 nm and a negative peak around 240 nm. After folding and treating with hemin, the CD profile of the BMAP18 C-PS5.M quadruplex showed induced CD bands in the 350−450 nm range (Figure S4A), attributed to the hemin noncovalently bound to the G4 and confirming the formation of a G4 structure. The same CD profile is confirmed for the GF17_His C-PS5.M analogue (Figure S4B).

As the conjugation yield of some of the AMP-G4 constructs was still very low, further improvements were required. Therefore, we used the sulfo-SMCC conjugation method but included an additional spacer comprising six thymines at the 5′-end of the oligonucleotide (Table S1, PS5.M_link, and

https://doi.org/10.1021/acsomega.5c10306
ACS Omega 2026, 11, 8024−8033

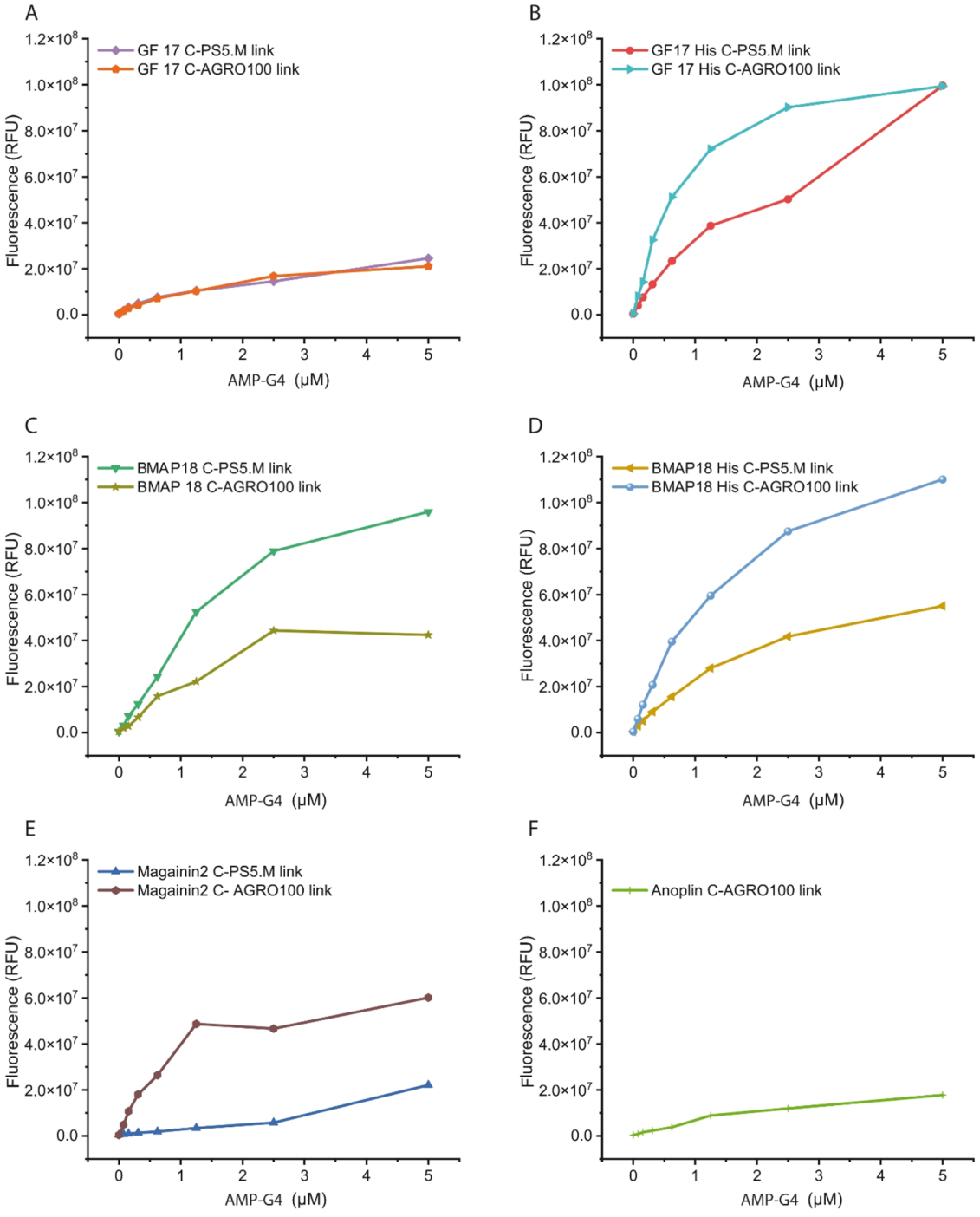

Figure 2. Interaction of different AMPs, including (A) GF17 C, (B) GF17 His C, (C) BMAP18 C, (D) BMAP18 His C, (E) Magainin C, and (F) Anoplin C, conjugated to G4 (either PS5.M or AGRO100) with a linker toward *E. coli* M/11407. The *X* and *Y* axes represent the fluorescence after excitation at 530 nm and emission at 590 nm and the concentration of the peptide (μM), respectively. The cells were immobilized at OD_{600} 1.

AGRO100_link). We hypothesized that an additional spacer could provide a better reactivity due to less pronounced steric hindrance. SDS-PAGE electrophoresis was used to visualize the products of the conjugation reactions (Figure S5).

After the successful formation of AMP-DNA conjugates was demonstrated by SDS-PAGE electrophoresis, and the HPLC analyses confirmed efficient conversion of the starting DNA oligonucleotides to AMP-DNA conjugates (Figure S7), the conjugates were subjected to DNAzyme folding. UV/vis and particularly CD spectroscopy were used to characterize the G4 component. The CD profiles of BMAP18 C-PS5.M_link and BMAP18 C-AGRO100_link conjugates after folding and treatment with hemin to form G4 structures displayed induced CD bands in the 350−450 nm range (Figure S6), confirming the formation of G4 structures.

Finally, the synthesized AMP-G4 products were tested for their enzymatic activity. As expected, the unfolded G4 was inactive, while after DNAzyme folding, it exhibited distinct catalytic activity (Figures S8C and S9F). Although the SPACC click reaction (*Experimental procedure 1*) resulted in low yields, we were still able to test the catalytic activity of some conjugates. BMAP18 His-PS5.M and PS5.M-His(N′)-

https://doi.org/10.1021/acsomega.5c10306
ACS Omega 2026, 11, 8024−8033

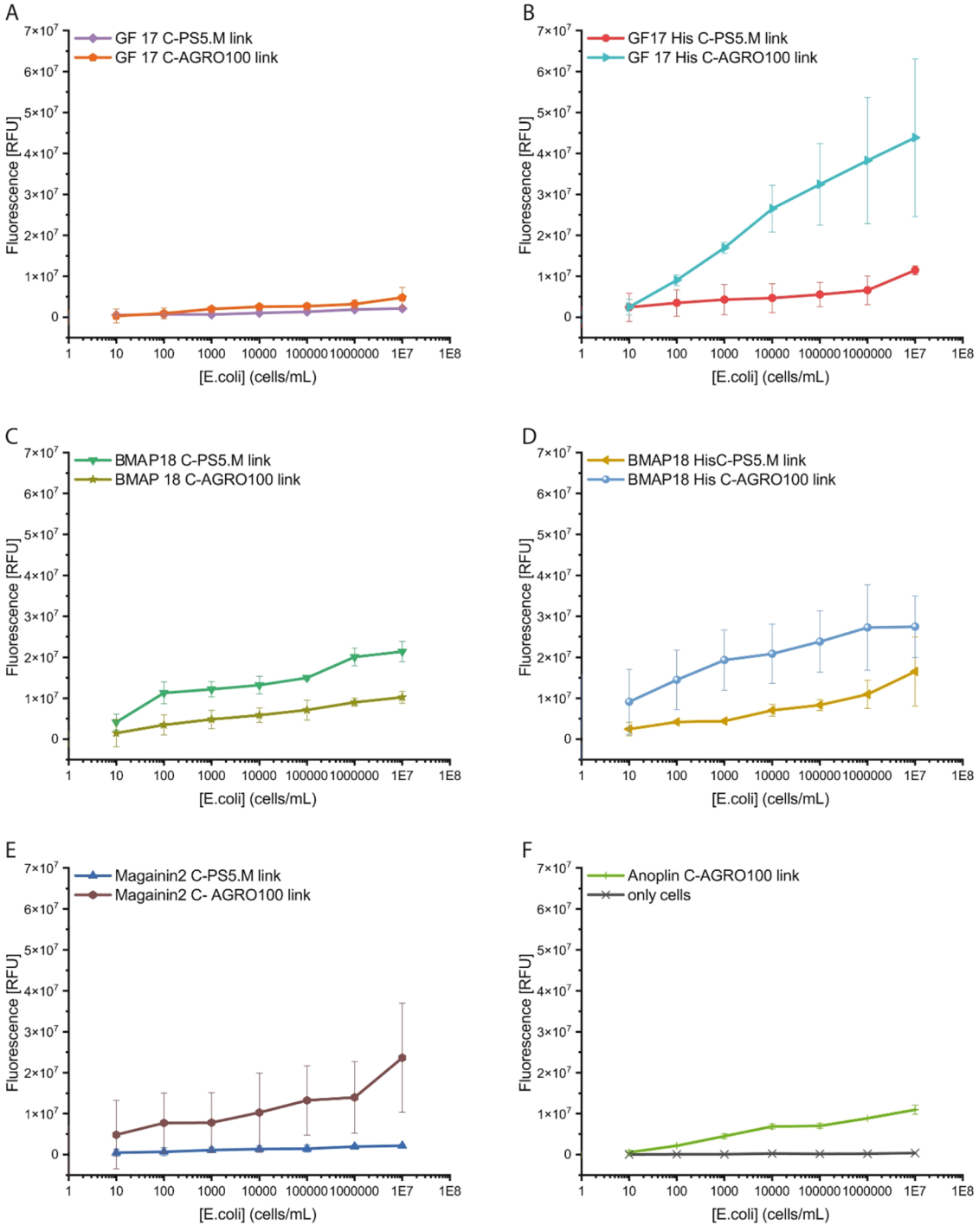

Figure 3. *E. coli* M/14072 cells were immobilized at different concentrations. Comparison of the effect of 5 μM AMPs conjugated to the G4 PS5.M or AGRO100 with linker (A) GF17 C, (B) GF17 His C, (C) BMAP18 C, (D) BMAP18 His C, (E) Magainin C, and (F) Anoplin C and PS5.M without AMP. The *X* and *Y* axes represent the fluorescence after excitation at 530 nm and emission at 590 nm and the concentration of *E. coli* M/14072 (cells/mL) shown in logarithmic scale, respectively. The data were blanked against wells without immobilized cells but blocked by BSA. Concentration of bacteria varied from 10 cells/mL to 10^9 cells/mL. All data blanked against the wells without immobilized cells.

Magainin2 showed a small increase in absorbance over time despite a low product formation efficacy. Presumably, steric hindrance not only inhibits the synthesis but also results in a reduced activity of the G4. Additionally, all AMP conjugates prepared by the sulfo-SMCC conjugation method comprising the T_6 linker were tested. All AMP-G4 constructs were catalytically active (Figures S8B and S9). In all cases, the AGRO100 conjugates possessed activity higher than that of the PS5.M conjugates. The presence of a His_5-tag had no effect for BMAP18 C but enhanced the activity considerably for GF17 C. As all constructs were active, we used all of them for the detection of bacteria.

3.2. Minimal Inhibitory Concentration (MIC) Experiments

AMPs can exert their bactericidal activity due to their high binding affinity for bacterial cell membranes. Once they are bound at high concentrations, they are capable of forming

https://doi.org/10.1021/acsomega.5c10306
ACS Omega 2026, 11, 8024−8033

pores or micelles, resulting in the rupture of the membrane and lysis of the bacteria. As we wanted to use the AMP-G4 construct to detect bacteria, AMPs should bind without killing the cells. We hypothesized that the conjugation of the AMP to the DNA reduces the lysis efficiency due to the charge repulsion of the negatively charged membrane and the DNA and steric hindrance. Therefore, we determined the MIC of the different AMP-G4 constructs. The results support our hypothesis, as the MIC for the tested peptides after conjugation to the DNA is at least four times higher than for the unmodified AMP (Table S3).

3.3. Detecting the Binding of AMP-G4 to *E. coli* on Syringe Filters

Recently, we presented a syringe filter-based bacterial detection platform.[19] However, it featured high background activity due to the nonspecific binding of HRP-streptavidin to the filter membranes. We hypothesized that our AMP-G4 conjugates could be a good alternative to such an HRP-streptavidin-based detection system. Therefore, we tested first whether the AMP-G4 conjugate itself can bind to the filter. As shown in Figures S10 and S11, no color development was observed in the absence of *E. coli* (OD_{600} 0) on polypropylene filters. Then, we performed experiments in which the filters were loaded with *E. coli* cells and subsequently 100 nM AMP-G4 conjugate, followed by the addition of a chromogenic substrate solution. In the presence of high concentrations of bacteria (OD_{600} 1, corresponding to 8×10^9 cells/mL), an intense blue color developed, indicating the binding of AMP-G4 to the cells. Even lower bacterial concentrations 4×10^8 (OD_{600} 0.5) could still be still detected. Reducing the concentration of bacteria further to an OD_{600} of 0.1 (ca. 8×10^7 cells/mL) resulted in no or very faint blue signals. With this detection system, the AMP-G4 with (Figure S10) and without a linker (Figure S11) performed similar. The G4 alone also induced color formation in the presence of bacteria, an effect that we have observed in our previous work.[17] While this filter-based detection method is simple and fast, it can detect only high concentrations of bacteria. Thus, we pursued the development of an ELISA-like assay to detect low bacterial concentrations.

3.4. Detecting the Binding of AMP-G4 to *E. coli* Using an ELISA-like Assay

Although some studies report that AMPs have species-specific binding properties, these cannot be exploited with our experimental setup.[27−29] Syringe filters and ELISA-like assays do not support multiplex detection approaches, and species-specific binding affinity differences cannot be differentiated from cell concentration effects. Thus, we opted to investigate the interaction of different AMP-G4 variants toward a single clinical *E. coli* strain. Therefore, cells were immobilized at an OD_{600} of 1. Then, different concentrations of our AMP-G4 constructs were applied, which bind via the peptide to the bacterial surface. The binding was detected by measuring the absorption or fluorescence resulting from the HRP-mimicking G4 after addition of substrate solution. First, the AMP-G4 constructs were tested with the commonly used TMB chromogenic substrate solution. The resulting colorimetric signal intensity was, however, low, even after 40 min reaction time (Figure S12). Thus, we changed to fluorescence measurements and used an Amplex Red fluorescent substrate. As is evident in Figure 2, for each peptide, a different combination of His-tag and G4 component leads to the best results.

3.5. Analyzing the Binding of AMP-G4 with Low *E. coli* Concentrations

To test if the AMP-G4 constructs are suitable to be used as a meaningful bacterial biosensor, we also tested low concentrations of cells by applying 5 μM AMP-G4 constructs to the detection reaction (Figure 3). To obtain quantitative data, we calculated the Limit of Detection (LoD), the lowest concentration that can be detected and reliably distinguished from the blank,[30] for each AMP-G4 construct. The data were fitted with linear equations (Figure S13), and the LoD was calculated (Table 1) as the average blank value plus three times the value of the standard deviation of the blank, converted to the concentration of bacteria. All but two constructs could bind to the bacterial surface with excellent LoD values of <100 cells/mL. However, the LoD of four constructs was outstanding. Magainin2 C-PS5.M link and Anoplin C-AGRO100 link have an LoD of less than 10 cells/ml, while GF17 His-AGRO100 link and BMAP18 C-AGRO100 link perform even better with an LoD of 4 cells/mL. Compared to most AMP-based biosensors, our best-performing constructs resulted in a 1−2 orders of magnitude higher sensitivity.[12]

Table 1. Limit of Detection (LoD) Values of the Investigated AMP-G4 Conjugates on *E. coli* M/14072

AMP-G4 conjugate	LoD [cells/mL]
GF17 C-PS5.M link	64
GF17 C-AGRO100 link	38
GF17 His-PS5.M link	1381
GF17 His-AGRO100 link	4
BMAP18 C-PS5.M link	77
BMAP18 C-AGRO100 link	4
BMAP18 His C-PS5.M link	125
BMAP18 His C-AGRO100 link	32
Magainin2 C-PS5.M link	7
Magainin2 C-AGRO100 link	501
Anoplin C-AGRO100 link	9

3.6. Molecular Dynamics Simulation of Selected AMP-G4 Constructs

Molecular dynamics (MD) simulations were conducted to elucidate the molecular basis behind the varying efficiency in bacterial detection among selected AMP-G4 conjugates. The analysis of structural and dynamic properties revealed two features that appear to be important for the efficient detection of bacterial cells: a high abundance of positively charged amino acids and the overall flexibility of the AMP.

The analysis of MD simulations showed that GF17 C maintains a stable and rigid α helix structure throughout the entire MD simulation (Figures S13 and S14), in which five positively charged amino acids are involved in H-bond interactions with G4 through the majority of the simulation. The AMP is oriented mostly toward G4 and the linker, hiding the positively charged amino acids from the solvent (Figure 4). Since positively charged amino acid residues of AMPs are necessary for interactions with the negatively charged bacterial membrane, this observation provides a possible explanation for the lower efficiency for bacterial detection of GF17 C.

Further, the results of MD simulations showed that the addition of five histidine residues on the C-terminus of GF17 C (system GF17 His C) led to a more flexible helical form (Figure S13). The presence of the His_5-tag increased the

https://doi.org/10.1021/acsomega.5c10306
ACS Omega 2026, 11, 8024−8033

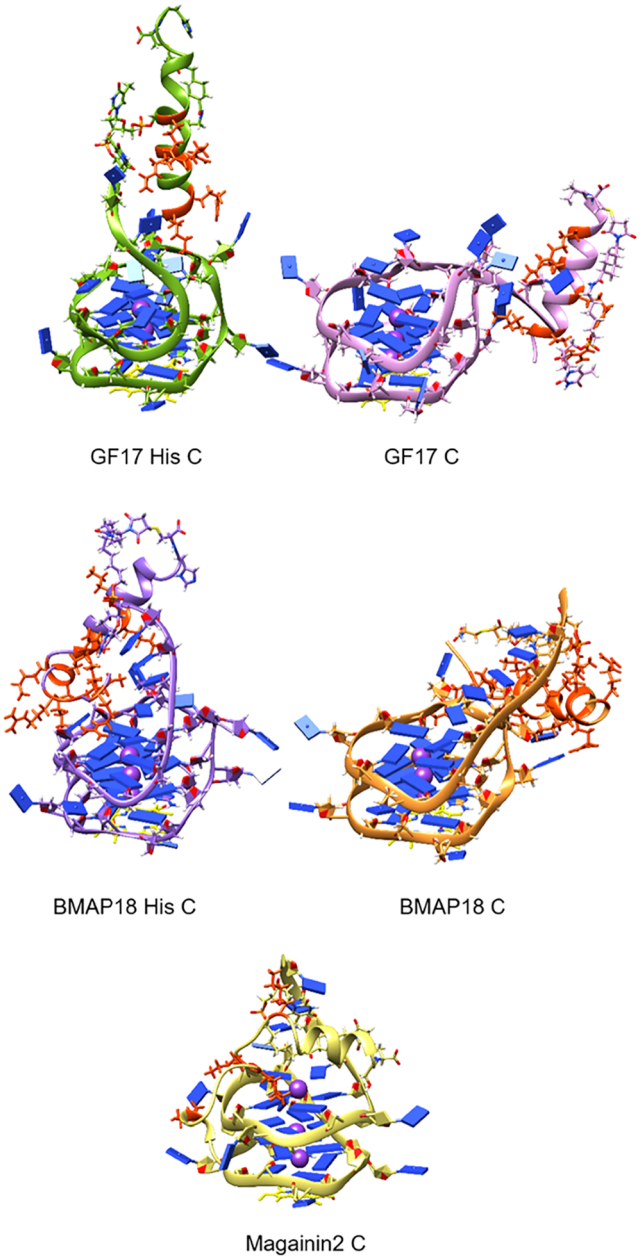

Figure 4. Most populated conformations obtained by the cluster analysis of MD simulations of GF17 C, GF17 His C, BMAP18 His C, BMAP18 C, and Magainin2 C conjugated to the AGRO100 G4. The linker structure is represented by sticks, while AMP and G4 are shown as ribbons. Positively charged amino acids are also shown as sticks and colored orange. K+ ions are shown as purple balls. Heme is depicted with yellow sticks.

flexibility of the AMP and caused the AMP helix to shift slightly away from the G4, which increased the exposure of positively charged amino acids to the solvent (Figure 4). This observation provides a possible molecular explanation for the experimentally observed increase of efficiency for bacterial detection due to the His_5-tag introduction (Figure 4). A similar effect of the His_5-tag introduction was observed through MD simulations of BMAP18 and BMAP18 His C. The addition of five histidine residues to BMAP18 increased the flexibility of AMP and caused occasional transitions between α and 3_{10} helix structures or unstructured turns at the N-terminus of AMP (Figures S13 and S14). Both BMAP18 and BMAP18 His C contain a considerable number of positively charged amino acids (10 in total, comprising three Arg and seven Lys, as detailed in Table S4). Despite numerous H-bond interactions that are established between these positively charged amino acids of the AMP and G4, many positively charged amino acids of the AMP remained available for interactions with the negatively charged bacterial membrane (Figure 4). Both BMAP18 and BMAP18 His C have a high efficiency for bacterial detection, but the presence of the His_5-tag increased the flexibility of the AMP and could be the reason for the increase in the efficiency for bacterial detection.

The results of MD simulations showed a high AMP flexibility of Magainin2 C and Apidaecin C. During MD simulations, the N-terminal residues of Magainin2 C exhibited high flexibility and occasional transitions between different helical forms (Figures S13, S14, and4). Apidaecin C showed the most structural flexibility, and its residues did not show any propensity toward forming secondary structures during the whole MD simulation (Figures S13, S14, and4). However, cluster analysis showed that in the most populated conformation of the trajectory, the AMP chain occluded the Fe^{2+} ion (Figure S14), which can lead to a decrease of the peroxidase activity.

4. CONCLUSIONS

We successfully prepared peptide-DNA conjugates using two strategies: (1) SPAAC click chemistry between azido-functionalized AMPs (via ISA·HCl) and DBCO-modified DNA, and (2) a site-selective sulfo-SMCC-based thiol−maleimide reaction that tethers DNA to a cysteine residue on the AMP. While the SPAAC approach yielded product mixtures due to multiple reactive amines, the sulfo-SMCC strategy enabled site-specific conjugation and was used to generate 14 distinct AMP−G4 constructs. These conjugates were evaluated on two detection platforms. In a fast, low-cost filter-based assay, AMP−G4 constructs could detect *E. coli* but only at high cell densities, whereas an ELISA-like assay, though more time-consuming, achieved limits of detection below 5 cells/mL with the best-performing constructs (GF17 His−AGRO100 and BMAP18 C−AGRO100). MD simulations indicated that the AMP positive charge and flexibility are key determinants of bacterial binding efficiency.

Several previous studies employed either AMPs or DNAzyme alone as the main component of their biosensing platform for bacterial detection. To the best of our knowledge, this is the first work in which these two were combined into one single, highly thermostable biosensor. Given the limited specificity of AMP binding to various bacterial species and strains, these biosensors can be useful in areas where broad safety assurance and cost-effectiveness are priorities. These include environmental monitoring (e.g., water quality testing), food safety, and quality control, where emphasis is on the presence of bacterial contamination, rather than identifying specific species. Taken together, our findings establish AMP−G4 DNAzyme conjugates as a promising and versatile platform for robust, low-cost bacterial biosensing and provide a solid basis for further optimization and application in real-world settings.

5. OUTLOOK

Future studies will focus on assessing the performance of AMP-G4 DNAzyme constructs across a broader panel of

https://doi.org/10.1021/acsomega.5c10306
ACS Omega 2026, 11, 8024−8033

bacterial isolates, including other clinically important pathogenic bacteria. Rational redesign of AMP sequences—guided by MD simulations and structure−activity relationships—could be used to fine-tune binding strength and selectivity. These conjugates could also be integrated into microfluidic or paper-based point-of-care platforms to enable miniaturized, low-cost, and user-friendly assays. Ultimately, evaluation in complex real-world matrices (e.g., food, environmental water, clinical specimens) and benchmarking against gold standard diagnostic methods will be essential to advance AMP−G4 biosensors toward robust, field-deployable platforms.

■ ASSOCIATED CONTENT

Supporting Information

The Supporting Information is available free of charge at https://pubs.acs.org/doi/10.1021/acsomega.5c10306.

Detailed descriptions of the synthesis of the AMP-G4 constructs, the molecular dynamics simulation, the sequences of all oligonucleotides, G4, and peptides (PDF)

■ AUTHOR INFORMATION

Corresponding Authors

Ivo Piantanida − *Division of Organic Chemistry and Biochemistry, Laboratory for Biomolecular Interactions and Spectroscopy, Ruđer Bošković Institute, 10000 Zagreb, Croatia*; Email: ivo.piantanida@irb.hr

Ivan Barišić − *Molecular Diagnostics, Center for Health and Bioresources, AIT Austrian Institute of Technology GmbH, 1210 Vienna, Austria; Eko Refugium, 47240 Slunj, Croatia*; orcid.org/0000-0002-1301-6197; Email: ivan.barisic@ait.ac.at

Authors

Natalie Mutter − *Molecular Diagnostics, Center for Health and Bioresources, AIT Austrian Institute of Technology GmbH, 1210 Vienna, Austria*; orcid.org/0000-0002-9144-7443

Filippo Savini − *Molecular Diagnostics, Center for Health and Bioresources, AIT Austrian Institute of Technology GmbH, 1210 Vienna, Austria*; orcid.org/0000-0001-7680-9242

Željka Ban − *Division of Organic Chemistry and Biochemistry, Laboratory for Biomolecular Interactions and Spectroscopy, Ruđer Bošković Institute, 10000 Zagreb, Croatia*

Dijana Pavlović Saftić − *Division of Organic Chemistry and Biochemistry, Laboratory for Biomolecular Interactions and Spectroscopy, Ruđer Bošković Institute, 10000 Zagreb, Croatia*

Andrea Hloušek-Kasun − *Department of Chemistry, Faculty of Science, University of Zagreb, Zagreb, HR 10000, Croatia*

Yasaman Ahmadi − *Molecular Diagnostics, Center for Health and Bioresources, AIT Austrian Institute of Technology GmbH, 1210 Vienna, Austria*

Branimir Bertoša − *Department of Chemistry, Faculty of Science, University of Zagreb, Zagreb, HR 10000, Croatia*; orcid.org/0000-0002-4540-5648

Complete contact information is available at: https://pubs.acs.org/10.1021/acsomega.5c10306

Author Contributions

N.M.: Investigation, formal analysis, and writing—original draft. F.S.: Investigation and, writing—original draft. Z.B.: Investigation. D.P.S.: Investigation and writing—review and editing. A.H.-K.: Investigation and formal analysis. Y.A.: Writing—review and editing. B.B.: Funding acquisition, supervision, and writing—review and editing. I.P.: Funding acquisition, supervision, writing—review and editing. I.B.: Funding acquisition, supervision, and writing—review and editing.

Notes

The authors declare no competing financial interest.

■ ACKNOWLEDGMENTS

This project has received funding from the European Union's Horizon 2020 research and innovation programme under grant agreement No. 952110. The authors thank Doris Rakoczy for proofreading the manuscript.

■ REFERENCES

(1) Ikuta, K. S.; Swetschinski, L. R.; Aguilar, G. R.; et al. Global mortality associated with 33 bacterial pathogens in 2019: a systematic analysis for the Global Burden of Disease Study 2019. *Lancet* **2022**, *400* (10369), 2221−2248, DOI: 10.1016/S0140-6736(22)02185-7.

(2) Abate, G.; Aseffa, A.; Selassie, A.; Goshu, S.; Fekade, B.; WoldeMeskal, D.; Miörner, H. Direct colorimetric assay for rapid detection of rifampin-resistant Mycobacterium tuberculosis. *J. Clin. Microbiol.* **2004**, *42* (2), 871−873.

(3) Mookherjee, N.; Anderson, M. A.; Haagsman, H. P.; Davidson, D. J. Antimicrobial host defence peptides: functions and clinical potential. *Nat. Rev. Drug discovery* **2020**, *19* (5), 311−332.

(4) Lazzaro, B. P.; Zasloff, M.; Rolff, J. Antimicrobial peptides: Application informed by evolution. *Science* **2020**, *368* (6490), No. eaau5480, DOI: 10.1126/science.aau5480.

(5) Bobone, S.; Stella, L. Selectivity of Antimicrobial Peptides: A Complex Interplay of Multiple Equilibria. *Adv. Exp. Med. Biol.* **2019**, *1117*, 175−214.

(6) Savini, F.; Luca, V.; Bocedi, A.; Massoud, R.; Park, Y.; Mangoni, M. L.; Stella, L. Cell-Density Dependence of Host-Defense Peptide Activity and Selectivity in the Presence of Host Cells. *ACS Chem. Biol.* **2017**, *12* (1), 52−56.

(7) Ahmadi, Y.; Savini, F.; Mutter, N.; Barišić, I. Application of Antimicrobial Peptides as Diagnostic Biosensors. *Anal. Chem.* **2024**, *96* (1), 256−264.

(8) Etayash, H.; Norman, L.; Thundat, T.; Stiles, M.; Kaur, K. Surface-conjugated antimicrobial peptide leucocin a displays high binding to pathogenic gram-positive bacteria. *ACS Appl. Mater. Interfaces* **2014**, *6* (2), 1131−1138.

(9) Dong, Z.-M.; Zhao, G.-C. Label-free detection of pathogenic bacteria via immobilized antimicrobial peptides. *Talanta* **2015**, *137*, 55−61.

(10) de Miranda, J. L.; Oliveira, M. D. L.; Oliveira, I. S.; Frias, I. A. M.; Franco, O. L.; Andrade, C. A. S. A simple nanostructured biosensor based on clavanin A antimicrobial peptide for gram-negative bacteria detection. *Biochem. Eng. J.* **2017**, *124*, 108−114.

(11) Yuan, K.; Mei, Q.; Guo, X.; Xu, Y.; Yang, D.; Sánchez, B. J.; Sheng, B.; Liu, C.; Hu, Z.; Yu, G.; Ma, H.; Gao, H.; Haisch, C.; Niessner, R.; Jiang, Z.; Jiang, Z.; Zhou, H. Antimicrobial peptide based magnetic recognition elements and Au@Ag-GO SERS tags with stable internal standards: a three in one biosensor for isolation, discrimination and killing of multiple bacteria in whole blood. *Chem. Sci.* **2018**, *9* (47), 8781−8795.

(12) Islam, M. A.; Karim, A.; Ethiraj, B.; Raihan, T.; Kadier, A. Antimicrobial peptides: Promising alternatives over conventional capture ligands for biosensor-based detection of pathogenic bacteria. *Biotechnol. Adv.* **2022**, *55*, No. 107901.

(13) Islam, M. A.; Hassen, W. M.; Tayabali, A. F.; Dubowski, J. J. Short Ligand, Cysteine-Modified Warnericin RK Antimicrobial Peptides Favor Highly Sensitive Detection of Legionella pneumophila. *ACS Omega* **2021**, *6* (2), 1299−1308.
(14) Islam, M. A.; Hassen, W. M.; Tayabali, A. F.; Dubowski, J. J. Antimicrobial warnericin RK peptide functionalized GaAs/AlGaAs biosensor for highly sensitive and selective detection of Legionella pneumophila. *Biochem. Eng. J.* **2020**, *154*, No. 107435.
(15) Sen, D.; Gilbert, W. Formation of parallel four-stranded complexes by guanine-rich motifs in DNA and its implications for meiosis. *Nature* **1988**, *334* (6180), 364−366.
(16) Sundquist, W. I.; Klug, A. Telomeric DNA dimerizes by formation of guanine tetrads between hairpin loops. *Nature* **1989**, *342* (6251), 825−829.
(17) Ahmadi, Y.; Soldo, R.; Rathammer, K.; Eibler, L.; Barišić, I. Analyzing Criteria Affecting the Functionality of G-Quadruplex-Based DNA Aptazymes as Colorimetric Biosensors and Development of Quinine-Binding Aptazymes. *Anal. Chem.* **2021**, *93*, 5161−5169.
(18) Khan, S.; Burciu, B.; Filipe, C. D. M.; Li, Y.; Dellinger, K.; Didar, T. F. DNAzyme-Based Biosensors: Immobilization Strategies, Applications, and Future Prospective. *ACS Nano* **2021**, *15* (9), 13943−13969.
(19) Savini, F.; Mutter, N.; Baumgartner, K.; Barišić, I. A Simple Biosensor Based on Streptavidin-HRP for the Detection of Bacteria Exploiting HRPs Molecular Surface Properties. *Appl. Biosci.* **2023**, *2* (3), 513−526.
(20) Pardoux, É.; Boturyn, D.; Roupioz, Y. Antimicrobial Peptides as Probes in Biosensors Detecting Whole Bacteria: A Review. *Molecules* **2020**, *25* (8), No. 1998.
(21) Guo, Y.; Wang, Y.; Liu, S.; Yu, J.; Wang, H.; Wang, Y.; Huang, J. Label-free and highly sensitive electrochemical detection of *E. coli* based on rolling circle amplifications coupled peroxidase-mimicking DNAzyme amplification. *Biosens. Bioelectron.* **2016**, *75*, 315−319.
(22) Pang, L.; Wang, L.'e.; Liang, Y.; Wang, Z.; Zhang, W.; Zhao, Q.; Yang, X.; Jiang, Y. G-triplex/hemin DNAzyme mediated colorimetric aptasensor for *Escherichia coli* O157:H7 detection based on exonuclease III-assisted amplification and aptamers-functionalized magnetic beads. *Talanta* **2024**, *269*, No. 125457.
(23) Ding, Y.; Zhang, Z.; Kaiyum, Y. A.; Heng, Y.; Johnson, P. E.; Liu, J. DNA aptamers for common buffer molecules: possibility of buffer interference in SELEX. *Org. Biomol. Chem.* **2024**, *22* (41), 8337−8343.
(24) Ban, Ž.; Barišić, A.; Crnolatac, I.; Kazazić, S.; Škulj, S.; Savini, F.; Bertoša, B.; Barišić, I.; Piantanida, I. Highly selective preparation of N-terminus Horseradish peroxidase-DNA conjugate with fully retained enzymatic activity: HRP-DNA structure - activity relation. *Enzyme Microb. Technol.* **2023**, *168*, No. 110257.
(25) Kut'ák, D.; Melo, L.; Schroeder, F.; Jelic-Matošević, Z.; Mutter, N.; Bertoša, B.; Barišić, I. CATANA: an online modelling environment for proteins and nucleic acid nanostructures. *Nucleic Acids Res.* **2022**, DOI: 10.1093/nar/gkac350.
(26) Melo, M. N.; Ferre, R.; Castanho, M. A. R. B. Antimicrobial peptides: linking partition, activity and high membrane-bound concentrations. *Nat. Rev. Microbiol.* **2009**, *7* (3), 245−250.
(27) Kulagina, N. V.; Lassman, M. E.; Ligler, F. S.; Taitt, C. R. Antimicrobial peptides for detection of bacteria in biosensor assays. *Anal. Chem.* **2005**, *77* (19), 6504−6508.
(28) Kulagina, N. V.; Shaffer, K. M.; Anderson, G. P.; Ligler, F. S.; Taitt, C. R. Antimicrobial peptide-based array for *Escherichia coli* and Salmonella screening. *Anal. Chim. Acta* **2006**, *575* (1), 9−15.
(29) Kulagina, N. V.; Shaffer, K. M.; Ligler, F. S.; Taitt, C. R. Antimicrobial peptides as new recognition molecules for screening challenging species. *Sens. Actuators, B* **2007**, *121* (1), 150−157.
(30) Gustavo González, A. G.; Ángeles Herrador, M. A. A practical guide to analytical method validation, including measurement uncertainty and accuracy profiles. *TrAC, Trends Anal. Chem.* **2007**, *26* (3), 227−238.

https://doi.org/10.1021/acsomega.5c10306
ACS Omega 2026, 11, 8024−8033